



Published in final edited form as:

Ophthalmol Retina. 2018 September ; 2(9): 963–971. doi:10.1016/j.oret.2018.02.001.

Spectral-Domain OCT Findings of Retinal Vascular-Avascular Junction in Infants with Retinopathy of Prematurity

Xi Chen, MD, PhD, Shwetha Mangalesh, MBBS, Alexandria Dandridge, Du Tran-Viet, BS, David K. Wallace, MD, MPH, Sharon F. Freedman, MD, and Cynthia A. Toth, MD
Department of Ophthalmology, Duke University, Durham, NC, 27710, USA

Abstract

PURPOSE—Bedside examination of premature infants at risk for retinopathy of prematurity (ROP) is predominantly performed with ophthalmoscopic *en face* viewing of the retina. While postmortem retinal microstructures have been studied at the vascular-avascular junction, a critical location for pathogenesis of ROP, to date this has not been possible *in vivo*. Here we present bedside, non-sedated *in vivo* cross-sectional imaging and analysis of retinal microstructures at the vascular-avascular junction in infants with ROP using handheld spectral-domain optical coherence tomography (SDOCT).

DESIGN—Prospective observational study.

PARTICIPANTS—Eleven preterm infants consented for research imaging during ROP screening examinations.

METHODS—We imaged the vascular-avascular junction in the temporal retina using a SDOCT system (Envisu, Bioptigen Inc., NC) in 18 eyes from 11 preterm infants with zone I or II, stage 0 through 4 ROP. B-scan and *en face* images were analyzed and compared to historical light micrographs.

MAIN OUTCOME MEASURES—SDOCT morphology at the vascular-avascular junction.

RESULTS—Multiple bedside SDOCT findings at the vascular-avascular junction were comparable to historic light micrographs: thickened inner retinal ridge structure in stage 2 ROP was comparable to thickened vanguard and rear guard cells in micrographs; vascular tufts on the posterior retinal surface in stage 2 ROP, broad arcs of neovascularization above the retina in stage 3 ROP, and splitting of inner retinal layers into clefts on either side of neovascularization

Corresponding Author: Cynthia A. Toth, M.D., Department of Ophthalmology, Duke University Medical Center, 2351 Erwin Road – Box 3802, Durham, NC 27710, Phone: 919-684-5631, Fax: 919-681-6474, cynthia.toth@dm.duke.edu.

Publisher's Disclaimer: This is a PDF file of an unedited manuscript that has been accepted for publication. As a service to our customers we are providing this early version of the manuscript. The manuscript will undergo copyediting, typesetting, and review of the resulting proof before it is published in its final citable form. Please note that during the production process errors may be discovered which could affect the content, and all legal disclaimers that apply to the journal pertain.

Meeting Presentation: Part of this manuscript was presented at the Association for Research in Vision and Ophthalmology (ARVO) 2016 annual meeting, the Retina Society 2016 annual meeting, and the American Association for Pediatric Ophthalmology and Strabismus (AAPOS) 2016 meeting.

Conflict of Interest: No other authors have financial disclosures. No authors have a proprietary interest in the current study.

This article contains additional online-only material. The following should appear online-only: Supplementary figure 1, supplementary table 1 and supplementary video 1.

mimicked findings of historic light micrographs. A unique findings was thickening of the avascular inner retinal band adjacent to neovascularization. On SDOCT imaging over several weeks, neovascularization and retinal clefts diminished after intravitreal bevacizumab therapy.

CONCLUSIONS—Retinal morphology at the vascular-avascular junction imaged with handheld SDOCT is consistent with known histopathology, and provide the advantage of monitoring change *in vivo* over time. These unique findings provide new insights into preterm retinal neurovascular development in ROP.

Introduction

With development of early perinatal care and increased survival of extremely preterm infants, retinopathy of prematurity (ROP) has become a leading cause of childhood blindness and subnormal vision in the United States.^{1–3} ROP is characterized by delayed and abnormal retinal vascular growth. Current standard of care for severe ROP (type 1 ROP) is laser treatment of the avascular retina, while intravitreal anti-VEGF therapy is rapidly gaining traction as an effective alternative treatment, especially in cases of aggressive posterior disease.^{4, 5}

Imaging in the pediatric population has historically been challenging due to limited access to examine the eyes of a supine infant in an intensive care nursery. The mainstay of widefield retinal imaging in the nursery has been Retcam fundus photography (Clarity Medical Systems, Inc., Pleasanton, CA, USA). Intravenous fluorescein angiography has been very useful to examine the vasculature and determine foveal center and staging in infants with ROP, but it is an invasive procedure for very preterm infants and does not elucidate non-vascular neural tissue layers.^{6–9} Ultra-widefield imaging with a tabletop system (Optos PLC, Dunfermline, UK) has been shown to be very informative in documentation of the fundus exam, however, it is difficult to achieve the “flying baby” position in a physically unstable preterm infant.¹⁰ The development of handheld spectral-domain optical coherence tomography (SDOCT) for pediatric use has provided significant insights into human retinal development.^{11–14} Implementation of this method overcame a major hurdle in neonatal retinal imaging, allowing visualization of cross-sectional neurovascular structures at the cellular level in infants who are unable to cooperate for traditional tabletop SDOCT imaging.^{11, 13, 15} Through bedside nursery imaging, researchers have identified atypical morphology, such as cystoid macular edema in preterm infants and subfoveal fluid in term infants, both of which were rarely noted by conventional indirect ophthalmoscopy.^{16, 17} However, bedside OCT imaging of the peripheral retina, where most pathology associated with ROP occurs, has been scarce. To date, retinoschisis-like changes in areas of attached retina have been reported on OCT imaging during examination under anesthesia of eyes of infants with severe ROP.^{18–20} In a more recent report, preretinal tissue was visualized on widefield handheld OCT in an infant after laser treatment for Type 1 ROP.²¹

Prior histopathological studies of ROP have been limited. ROP, initially known as “retrolental fibroplasia”, was first described by Terry in 1942.^{22, 23} Initial pathology studies focused on late changes of the disease, characterized by funnel retinal detachment and massive retrolental fibrosis. It was not until the 1950s that changes in histopathology during

earlier stages of the disease were described in detail.^{24–30} These findings formed the basis of what we now understand as an entity of abnormal vascular proliferation, which were further characterized and organized into various stages by Foos in 1978.³¹ The retinal microstructure at the location of the vascular-avascular junction, however, has been poorly defined in the literature, largely due to the inability to capture a simultaneous cross-section and *en face* image during eye examination or in histopathology studies. Thus, localization of a particular pathology section was difficult and could not be correlated with direct clinical observation.

Here we reported bedside, non-sedated, noncontact, *in vivo* imaging of the development of peripheral retinal layers, vessels and neovascularization across the vascular-avascular junction in infants with ROP using a handheld SDOCT imaging system, with correlation of the OCT findings with conventional clinical examination. We also correlated the stages of development at the vascular-avascular junction on SDOCT with data from previously published histopathology studies.^{24–28, 30–33} Many of these retinal changes were not evident on indirect ophthalmoscopy exams. We further identified response of neovascularization at the vascular-avascular junction after intravitreal bevacizumab therapy for clinically-diagnosed type 1 ROP.

Methods

The current descriptive pilot study was part of a larger, prospective study of retinal development that was approved by the Duke University Health System institutional review board and adheres to the Health Insurance Portability and Accountability Act and all tenets of the Declaration of Helsinki. All preterm infants were enrolled from January 2014 through May 2017 with parent or legal guardian written informed consent to participate in this research study. For the current study, we included a subset of 18 eyes from 11 preterm infants imaged over 30 sessions (out of a group of 55 infants with zone I or II, stage 0 through 4 ROP), in whom we pursued peripheral imaging of the vascular-avascular junction. Some of these infants had received prior laser or anti-VEGF treatments as clinically indicated. Poor quality scans, due to poor signal quality or inability to view the vascular-avascular junction, were excluded. The participants' medical records were reviewed for gestational age and general health information. All infants were imaged following the standard clinical examination and screening for ROP, which included dilated fundus examination using indirect ophthalmoscopy. The staging of ROP was based on standard bedside indirect ophthalmoscopy examination and annotation on a standard International Classification of Retinopathy of Prematurity (ICROP) diagram³⁴ by experienced pediatric ophthalmologists at Duke University Hospital (SFF or DKW).

The SDOCT images were captured at the time of ROP examination using a handheld device on neonates in a supine position in the isolette. The average pupil size was 6 mm and infants did not fixate on a target. SDOCT imaging was performed according to an age-specific protocol described by Maldonado et al using the portable handheld SDOCT system (Bioptigen, Inc, Research Triangle Park, North Carolina, USA).³⁵ Capture time for each volume was about 1.2 seconds. Approximately 10–25 volumes were obtained per imaging session within the allowed time for research imaging (15 minutes), with the goal of

capturing perpendicular scans through the vascular-avascular junction in the temporal retina after completing standard scans of the macula and optic nerve head. In general, eyes with zone I and posterior zone II diseases were imaged and included for analysis. The vascular-avascular junction was defined by tracing the end of peripheral vasculature on the *en face* retinal images (summed-voxel projection (SVP) images), and the corresponding location was marked on the correlated B-scans. Some of the borders of vascular-avascular junction was difficult to determine, especially in areas of detached retina. This was done in comparison of other imaging modalities (such as Retcam images) near the time of bedside imaging. The inner and outer retinal microstructural changes were examined during different stages of ROP. Retinal and choroidal thickness of the vascular-avascular junction was measured on the OCT B-scan images. Retinal thickness at 1000 μm anterior or posterior to the vascular-avascular junction was also measured using calipers on the Biotigen Envisu viewing software. The OCT B-scan images were denoised using custom Matlab scripts and/or enhanced by averaging three adjacent consecutive scans.

SDOCT images at the vascular-avascular junction from this study were compared to light micrographs from prior publications that addressed the vascular-avascular junction in ROP (included in Figure 3, right panels).^{28, 31, 33} We searched for relevant publications of retrolental fibroplasia or retinopathy of prematurity with light micrographs that might include the vascular-avascular junction. SDOCT images were compared to the published light micrographs at corresponding stages of ROP and of vascular development with reproduced and adapted images from Reese et al 1952, Kushner et al 1977 and Foos 1987.

A literature search of the PubMed database on July 14th, 2017 for “retinopathy of prematurity” and “OCT” did not identify publications that addressed the vascular-avascular junction in infants.

Results

We captured good quality peripheral OCT imaging of the vascular-avascular junction in the temporal retina in 18 eyes from 11 preterm infants with zone I or II, stage 0 through 4 ROP using the handheld SDOCT system in non-sedated infants in the neonatal intensive care unit (NICU) or transitional care nursery (TCN). Of the 18 eyes, 11 had good quality scans from one visit and 7 had good quality scans from 2 or more visits. The demographics, stages of ROP, gestational age at birth and postmenstrual age (PMA) at exam, and prior treatments of these infants are summarized in Table 1.

A montage of the retinal projections from numerous SDOCT volumes covering the posterior pole and temporal peripheral retina including the vascular-avascular junction in a 35-week (PMA) infant born at 24 weeks with zone II stage 3 ROP is shown in Figure 1 for orientation. From these volumes, OCT B-scans could be extracted for examination while maintaining *en face* localization and orientation as shown in the two examples. First, in a B-scan of the macula, we found absence of subfoveal photoreceptor ellipsoid zone, typical of a preterm infant fovea at this age^{11, 13} (Figure 1, star). Second, in a B-scan of the temporal peripheral retina, we found preretinal neovascular elevations (Figure 1, arrowhead) at the vascular-avascular junction and inner retinal thickening of the anterior avascular retina

(Figure 1, arrow). Imaging at both the macula and the temporal peripheral retina was reviewed. Macular imaging showed cystoid macular edema in 9/18 eyes and preretinal neovascular tissue in 7/18 eyes. The sample size is too small to correlate the OCT findings at the macula and the retinal periphery.

Retinal microstructural changes at the vascular-avascular junction on OCT and histopathology

Inner retinal structures changed notably in transition from vascularized retina to avascular retina on B-scan images, while outer retinal structures remained similar across the vascular-avascular junction (Figure 2). The inner retinal structures differed corresponding to the stages of ROP, with unique appearances of neural and vascular tissue at the vascular-avascular junction with each stage of ROP greater than stage 1. These findings paralleled the previously published light micrographs from rare postmortem tissue.^{28, 31, 33} Findings at the vascular-avascular junction on OCT by ROP stage were as follows.

Stage 0–1—In two eyes with stage 0 and one eye with stage 1 ROP, the vascularized retina posterior to the vascular-avascular junction was composed of a three-layered inner retina with hyperreflective bands on either side of a hyporefective layer (Figure 2A). The avascular retina anterior to the vascular-avascular junction, in contrast, exhibited a single hyperreflective band in the inner retina (Figure 2A). The outer retinal layer appeared as a broad hyporefective band in both vascularized and avascular peripheral retina. Within the broader hyporefective band, a thin, hyperreflective band was sometimes visible (Figure 2A). There was no significant difference in the outer retinal structures and the retinal pigment epithelium across the vascular-avascular junction. The choroidal was readily visible on most scans, but no consistent change in thickness was observed across the junction (Figure 2A, Supplementary Table 1). The retinal microstructure were relatively indistinguishable between the eyes with stage 0 and stage 1 ROP, except that the total retinal thickness of the vascularized retina (measured from the retinal surface to the RPE band 1000 μm posterior to the vascular-avascular junction) appeared to be greater in the stage 1 eye compared to the stage 0 eye (Supplementary Table 1). However, this observation was speculative and remained to be demonstrated in a larger study.

Previously published histopathology studies of the peripheral retina in stage 0 ROP were extremely limited. Foos described normal retinal angiogenesis as two active zones by microscopy, an anterior vanguard containing spindle-shaped cells, and a posterior rear guard containing primitive endothelial cells (Figure 3A).³¹ These microstructural changes were not evident on OCT B-scans. In contrast, OCT identified a three-layered inner retina, which may reflect the horizontally-oriented cells in the ganglion cell layer as shown on histopathology sections (Figure 3A). In prior histopathology studies of infants with stage 1 ROP, a thicker inner retinal layer has been reported with hyperplasia of the primitive spindle-shaped cells at the demarcation line (Figure 3B). The OCT finding paralleled these findings, but the hyperplastic change in the inner retina was not as obvious.

Stage 2—In one eye with stage 2 ROP (two separate imaging sessions one week apart), although the posterior vascularized retina was composed of a similar three-layered structure

on OCT, as we followed it anteriorly toward the vascular-avascular junction, the inner hyperreflective band became more thickened and homogenous, forming an elevated “ridge” at the temporal periphery (Figure 2C). This ridge was prominent throughout all OCT B-scans in the captured volume (unenhanced original B-scans, supplementary video 1). The edge of the elevated ridge ended slightly anterior to the vascular-avascular junction. The anterior avascular retina remained a thin hyperreflective band. The outer retinal layers, RPE and choroid, again, remained unchanged across the junction (Figure 2C). Prior histopathological findings of the ridge structure was closely imitated by the OCT B-scan findings (Figure 3C), as evident by a pronouncedly thickened epiretinal ridge consisting of hypertrophied vanguard and rear guard tissue with endothelial cell proliferation.³¹

Interestingly, in some stage 2 ROP scans, small tufts of elevated preretinal tissue were observed on OCT, which were not recognized by indirect ophthalmoscopy (Figure 3D). This also paralleled prior histopathology findings, which were described as small preretinal nests of endothelial cells.²⁸ This finding may be the earliest extraretinal pathological endothelial proliferative activity in an infant with clinical stage 2 ROP. When visible by indirect ophthalmoscopy, these extraretinal tissue tufts are often called “popcorn”.^{34, 36}

Stage 3—In six eyes/imaging sessions with stage 3 ROP and eight eyes/sessions with regressed ROP, OCT imaging revealed frequent neovascular tufts, buds and bands extending from the inner retinal surface posterior to the vascular-avascular junction. These preretinal structures appeared to coalesce and terminate around the location of the vascular-avascular junction (Figure 2D). The inner retinal layer in the anterior avascular region had developed into a significantly thickened hyperreflective band, in contrast to the now thinner inner layer of the posterior vascularized retina. The outer retinal layers, RPE and choroid still appeared unchanged across the junction (Figure 2D). The preretinal neovascular elevations observed on OCT imaging were consistent with what was observed in prior histopathology studies, in which neovascular tissue, observed in a budding form (Figure 3E) or in meshwork form (Figure 3F), was hypothesized to be retina vessels breaking through the internal limiting membrane and sprouting from the retinal surface.²⁸ An inner retinal split, a lucent space within the inner retinal hyperreflective band, was sometimes visualized anterior to (Figure 4A), at (Figure 4B), or posterior to (Figure 4C) the vascular-avascular junction in stage 3 ROP. Focal vitreous traction leading to a larger area of retinoschisis, with separation of the inner retinal layer, was also observed in selected sections (Figure 4D).

Stage 4—In three eyes with stage 4 ROP, the vascular-avascular junction was difficult to distinguish due to presence of retinal detachment, retinoschisis and overlying preretinal tissue. Detached retina was captured with apparent vitreous traction near the vascular-avascular junction (Figure 2E). There were some laser scars and outer retinal atrophy that extended beyond the vascular-avascular junction (data not shown). In attached retina in the posterior pole, retinoschisis-like changes are frequently observed (Figure 3G). Historical histopathology sections of such retinal detachment and schisis-like changes were seldom reported. There was only one morphologically similar light micrograph identified in our literature search (Figure 3G).³³

Longitudinal response to anti-VEGF treatment

Preterm infants with stage 3 ROP in our study frequently exhibited preretinal neovascular elevations on OCT imaging that regressed after laser treatment or intravitreal bevacizumab injection for type 1 ROP. We imaged the same location at the vascular-avascular junction in the temporal peripheral retina prior to and three weeks after intravitreal bevacizumab injection in an infant with zone I, stage 3 ROP with plus disease. The matchup of these locations was confirmed by vascular patterning (Supplementary Figure 1). Prior to bevacizumab injection, the inner retinal layer was thickened and elevated with neovascular buds and bands at the vascular-avascular junction. A focal inner retinal lucency posterior to and at the vascular-avascular junction, as well as a thickened anterior inner retinal layer were observed (Figure 5A). Three weeks after a single dose of intravitreal bevacizumab injection, OCT imaging of the same location of the temporal peripheral retina showed significant reduction of inner retinal thickness. The previously observed robust preretinal neovascular elevations reduced to smaller foci of wispy preretinal tissue immediately above the inner retinal surface. A three-layered inner retina, with hyperreflective bands on either side of a hyporefective band, was now observed, and extended beyond the prior location of the vascular-avascular junction (Figure 5B). These observations were consistent with clinical regression of the neovascular tissue, as well as further vascularization of the peripheral retina.

Discussion

We visualized *in vivo* in cross-section retinal neurovascular microstructures at the vascular-avascular junction during different stages of ROP with less than 6 μm axial resolution on SDOCT imaging. Figure 6 represents schematically the stages of ROP as visualized by SDOCT. In early stages of ROP, the vascularized retina appeared to become slightly more thickened from stage 0 to stage 2 and taper to a peripheral thinner avascular inner retina, while a prominent inner retinal ridge became evident in stage 2 ROP. The avascular retina, while thin in stage 0 through 2 ROP, was significantly thickened in stage 3 ROP. Preretinal neovascular tissue was visible as buds and bands in later stages. Outer retinal structures, RPE and choroid remained unchanged across the vascular-avascular junction. After bevacizumab treatment, the preretinal neovascular tissue regressed, along with progression of intraretinal vascularization into previously avascular retina. Figure 6, as with all clinical staging of ROP, takes a continuous process and assigns it to clinically-relevant stages. It is important to recognize the range of neurovascular development within each stage. With the precision of OCT cross-sectional imaging, we may find it possible to further subcategorize the developing retina in preterm infants, such as a late stage 2 with small posterior vascular elevations, and an early stage 3 with thickening of the avascular inner retina.

This report represents visualization and morphology-to-histopathology correlation of the retinal neurovascular microstructures at the vascular-avascular junction in eyes of premature infants with various stages and severity of ROP. In histopathology studies, retinal structures were often challenging to orient relative to the vascular-avascular junction, largely due to the difficulty in identification of the junction based on a cross-sectional view. Our use of SDOCT volumes and the retinal projection view provided an opportunity to visualize

peripheral retina both *en face* and in cross-section, enabling the comparison of the microstructural changes in vascularized and avascular retina during different stages of ROP. We identified parallel OCT findings for most previously published light micrographs, some of which were shown in Figure 3. Notably, prior histopathology studies identified the “ridge” as a critical structure in distinguishing pathological from normal retinal vascularization, and delineated the vascular-avascular junction.^{24, 31, 37} In our study, the ridge structure in cross-section was quite prominent in stage 2 ROP, while it was not readily identifiable without an *en face* view in stage 0 or 1 ROP. This dramatic change in vascular-avascular junction to an elevated ridge seemed to be associated with an acceleration of pathological activity, possibly responding to a significant increase in the drive for abnormal neovascularization and increased level of VEGF.

Retinal microstructures readily visible on OCT imaging but not consistently seen on clinical indirect ophthalmoscopy during ROP screening included small neovascular budding posterior to the vascular-avascular junction in stage 2 ROP, and inner retinal lucency that frequently appeared around the locations of the vascular-avascular junction in stage 3 ROP. The small neovascular buds on the inner retinal surface in stage 2 ROP were similar to, but smaller than those observed during stage 3 ROP, and may represent a form fruste of what the clinician would term “popcorn” once visible on ophthalmoscopy.³⁶ These, in fact, may be the earliest pathological changes indicating possible progression to more advanced diseases. Inner retinal layer split, morphologically distinct from the hyporeflective band dividing the hyperreflective inner retina, was often observed anterior to, at, or posterior to the vascular-avascular junction in eyes with stage 3 ROP. The only relevant previously published histopathology study was the intercommunicating cystic spaces found in the avascular retina bordered by Mueller cells, which may or may not be its corresponding histopathology finding.³³ The clinical significance of this inner retinal split is unknown, but could be speculated to represent early stages of retinoschisis from focal vitreoretinal traction or from fluid exudation associated with pathological neovascularization. Only two previously published reports, conducted in the operating room prior to pars plana vitrectomy, attempted *in vivo* imaging of the retinal periphery and found retinoschisis-like changes extending into the macula in infants with advanced ROP.²⁰ We observed similar schisis-like changes in the setting of clinically-determined stage 4 ROP, extending from avascular retina into areas posterior to vascular-avascular junction and posterior to the area of retinal detachment. Future studies with focus on the vitreoretinal interface will yield insights into the timing and etiology of these observed changes in the retinal microstructures.

Dramatic differences in the thickness of avascular retina were noted in eyes with stage 3 ROP, compared to stage 0 through 2 ROP, and was another feature not obvious on clinical examination. This finding was accompanied by prominent neovascular elevations, either in singular budding form or coalesced meshwork form. The etiology underlying such thickening of the inner retinal layer of the avascular retina in more advanced ROP remains unclear; however, given the observed homogeneity of the inner retinal band, it could represent nerve fiber layer edema. This thickening of avascular retina could also be a sign of ischemia or uniform traction from the vitreous body, and may predict impending worsening of ROP.

OCT imaging now gives us the ability to follow temporal changes in retinal structures *in vivo*. Notably, we observed regression of epiretinal neovascular tissue and further vascularization of the previous avascular retina over a three-week period in an infant with zone I stage 3 ROP after treatment with intravitreal bevacizumab. Indeed, we visualized the continued development of a three-layered inner retina, and significant decrease in the dramatic extraretinal neovascular elevations to remnant preretinal tissue after bevacizumab treatment and a concurrent resolution of the inner retinal split. A benefit of non-invasive, bedside imaging, this ability to follow temporal changes in the retina is likely to yield new insights into retinal neural and vascular development in the future.

Our study is a pilot study in a small group of infants to demonstrate feasibility and limitations of bedside, non-sedated, *in vivo* SDOCT imaging of the vascular-avascular junction during ROP. Obtaining peripheral imaging using the current SDOCT system is achievable but difficult even in the most technically-experienced hands (acquisition of peripheral OCT images in zone 1 was easier than zone 2, yet image quality, when obtained, was comparable in both zones). Localization of a particular peripheral scan to a specific location of the retina is also challenging. A wider-field lens and a higher-speed swept-source OCT system are currently under development to improve the feasibility and accessibility of imaging the peripheral retina in an infant. Some of these infants with advanced ROP had prior treatments with bevacizumab and/or peripheral laser retinopexy, as noted in Table 1, which may affect our ability to compare what we observed with spontaneous regression of ROP in cases not severe enough to require treatment. Our study is limited by the small sample size, treatment heterogeneity, and ROP grading by a single examiner, albeit a senior expert. Future technical advancements, such as higher speed and wide-angle OCT scanning, and possible combination with OCT angiography will further characterize how the vascular-avascular junction develops normally and progresses through different stages of ROP, as well as its response to medical and surgical interventions.

Supplementary Material

Refer to Web version on PubMed Central for supplementary material.

Acknowledgments

Financial Support: Bayer global ophthalmology awards program (GOAP) fellowship project award; The Hartwell Foundation; The Andrew Family Charitable Foundation; Research to Prevent Blindness; Grant Number 1UL1RR024128-01 from the National Center for Research Resources (NCRR), a component of the National Institutes of Health (NIH), and NIH Roadmap for Medical research, Grant Number P30 EY001583 from the National Eye Institute (NEI), and Grant Number 1RO1 EY025009 from NIH. The sponsor or funding organizations had no role in the design or conduct of this research.

Dr. Toth receives royalties through her university from Alcon and research support from Biotigen and Genentech. She also has unlicensed patents pending in OCT imaging and analysis.

References

1. Palmer EA, Flynn JT, Hardy RJ, et al. Incidence and early course of retinopathy of prematurity. The Cryotherapy for Retinopathy of Prematurity Cooperative Group. *Ophthalmology*. 1991; 98(11): 1628–40. [PubMed: 1800923]

2. Quinn GE, Dobson V, Barr CC, et al. Visual acuity in infants after vitrectomy for severe retinopathy of prematurity. *Ophthalmology*. 1991; 98(1):5–13. [PubMed: 2023732]
3. Tasman W. Retinopathy of prematurity: do we still have a problem?: the Charles L. Schepens lecture. *Arch Ophthalmol*. 2011; 129(8):1083–6. [PubMed: 21825195]
4. Hartnett ME. Vascular endothelial growth factor antagonist therapy for retinopathy of prematurity. *Clin Perinatol*. 2014; 41(4):925–43. [PubMed: 25459781]
5. Mintz-Hittner HA, Kennedy KA, Chuang AZ, Group B-RC. Efficacy of intravitreal bevacizumab for stage 3+ retinopathy of prematurity. *N Engl J Med*. 2011; 364(7):603–15. [PubMed: 21323540]
6. Purcaro V, Baldascino A, Papacci P, et al. Fluorescein angiography and retinal vascular development in premature infants. *J Matern Fetal Neonatal Med*. 2012; 25(Suppl 3):53–6.
7. Klufas MA, Patel SN, Ryan MC, et al. Influence of Fluorescein Angiography on the Diagnosis and Management of Retinopathy of Prematurity. *Ophthalmology*. 2015; 122(8):1601–8. [PubMed: 26028345]
8. Patel SN, Klufas MA, Ryan MC, et al. Color fundus photography versus fluorescein angiography in identification of the macular center and zone in retinopathy of prematurity. *Am J Ophthalmol*. 2015; 159(5):950–7. e2. [PubMed: 25637180]
9. Lepore D, Molle F, Pagliara MM, et al. Atlas of fluorescein angiographic findings in eyes undergoing laser for retinopathy of prematurity. *Ophthalmology*. 2011; 118(1):168–75. [PubMed: 20709401]
10. Patel CK, Fung TH, Muqit MM, et al. Non-contact ultra-widefield imaging of retinopathy of prematurity using the Optos dual wavelength scanning laser ophthalmoscope. *Eye (Lond)*. 2013; 27(5):589–96. [PubMed: 23519279]
11. Maldonado RS, O'Connell RV, Sarin N, et al. Dynamics of human foveal development after premature birth. *Ophthalmology*. 2011; 118(12):2315–25. [PubMed: 21940051]
12. Hendrickson A, Possin D, Vajzovic L, Toth CA. Histologic development of the human fovea from midgestation to maturity. *Am J Ophthalmol*. 2012; 154(5):767–78. e2. [PubMed: 22935600]
13. Vajzovic L, Hendrickson AE, O'Connell RV, et al. Maturation of the human fovea: correlation of spectral-domain optical coherence tomography findings with histology. *Am J Ophthalmol*. 2012; 154(5):779–89. e2. [PubMed: 22898189]
14. Chavala SH, Farsiou S, Maldonado R, et al. Insights into advanced retinopathy of prematurity using handheld spectral domain optical coherence tomography imaging. *Ophthalmology*. 2009; 116(12):2448–56. [PubMed: 19766317]
15. Dubis AM, Subramaniam CD, Godara P, et al. Subclinical macular findings in infants screened for retinopathy of prematurity with spectral-domain optical coherence tomography. *Ophthalmology*. 2013; 120(8):1665–71. [PubMed: 23672969]
16. Cabrera MT, Maldonado RS, Toth CA, et al. Subfoveal fluid in healthy full-term newborns observed by handheld spectral-domain optical coherence tomography. *Am J Ophthalmol*. 2012; 153(1):167–75. e3. [PubMed: 21925640]
17. Maldonado RS, O'Connell R, Ascher SB, et al. Spectral-domain optical coherence tomographic assessment of severity of cystoid macular edema in retinopathy of prematurity. *Arch Ophthalmol*. 2012; 130(5):569–78. [PubMed: 22232366]
18. Campbell JP, Nudleman E, Yang J, et al. Handheld Optical Coherence Tomography Angiography and Ultra-Wide-Field Optical Coherence Tomography in Retinopathy of Prematurity. *JAMA Ophthalmol*. 2017
19. Joshi MM, Trese MT, Capone A Jr. Optical coherence tomography findings in stage 4A retinopathy of prematurity: a theory for visual variability. *Ophthalmology*. 2006; 113(4):657–60. [PubMed: 16581425]
20. Muni RH, Kohly RP, Charonis AC, Lee TC. Retinoschisis detected with handheld spectral-domain optical coherence tomography in neonates with advanced retinopathy of prematurity. *Arch Ophthalmol*. 2010; 128(1):57–62. [PubMed: 20065217]
21. Campbell JP, Nudleman E, Yang J, et al. Handheld Optical Coherence Tomography Angiography and Ultra-Wide-Field Optical Coherence Tomography in Retinopathy of Prematurity. *JAMA Ophthalmol*. 2017; 135(9):977–81. [PubMed: 28750113]

22. Terry TL. Fibroblastic Overgrowth of Persistent Tunica Vasculosa Lentis in Infants Born Prematurely: II. Report of Cases—Clinical Aspects. *Trans Am Ophthalmol Soc.* 1942; 40:262–84. [PubMed: 16693285]
23. Terry TL. Retroental fibroplasia. *J Pediatr.* 1946; 29(6):770–3. [PubMed: 20277990]
24. Ashton N. Pathological basis of retroental fibroplasia. *Br J Ophthalmol.* 1954; 38(7):385–96. [PubMed: 13172416]
25. Friedenwald JS, Owens WC, Owens EU. Retroental fibroplasia in premature infants. III. The pathology of the disease. *Trans Am Soc Ophthalmol Otolaryngol Allergy.* 1951; 49:207–34. [PubMed: 14922441]
26. Heath P. Pathology of the retinopathy of prematurity: retroental fibroplasia. *Am J Ophthalmol.* 1951; 34(9):1249–59. [PubMed: 14877946]
27. Reese AB, Blodi FC. Retroental fibroplasia. *Am J Ophthalmol.* 1951; 34(1):1–24. [PubMed: 14799575]
28. Reese AB, Blodi FC, Locke JC. The pathology of early retroental fibroplasia, with an analysis of the histologic findings in the eyes of newborn and stillborn infants. *Am J Ophthalmol.* 1952; 35(10):1407–26. [PubMed: 12985788]
29. Vrabec TR, McNamara JA, Eagle RC Jr, Tasman W. Cryotherapy for retinopathy of prematurity: a histopathologic comparison of a treated and untreated eye. *Ophthalmic Surg.* 1994; 25(1):38–41. [PubMed: 8152731]
30. Ward BA. Ocular histology in premature infants with reference to retroental fibroplasia. *Br J Ophthalmol.* 1954; 38(8):445–59. [PubMed: 13182164]
31. Foos RY. Retinopathy of prematurity. Pathologic correlation of clinical stages. *Retina.* 1987; 7(4): 260–76. [PubMed: 2448856]
32. Hendrickson A. Development of Retinal Layers in Prenatal Human Retina. *Am J Ophthalmol.* 2015
33. Kushner BJ, Essner D, Cohen IJ, Flynn JT. Retroental Fibroplasia. II. Pathologic correlation. *Arch Ophthalmol.* 1977; 95(1):29–38. [PubMed: 576397]
34. International Committee for the Classification of Retinopathy of P. The International Classification of Retinopathy of Prematurity revisited. *Arch Ophthalmol.* 2005; 123(7):991–9. [PubMed: 16009843]
35. Maldonado RS, Izatt JA, Sarin N, et al. Optimizing hand-held spectral domain optical coherence tomography imaging for neonates, infants, and children. *Invest Ophthalmol Vis Sci.* 2010; 51(5): 2678–85. [PubMed: 20071674]
36. Wallace DK, Kylstra JA, Greenman DB, Freedman SF. Significance of isolated neovascular tufts ("popcorn") in retinopathy of prematurity. *J AAPOS.* 1998; 2(1):52–6. [PubMed: 10532368]
37. Gariano RF. Special features of human retinal angiogenesis. *Eye (Lond).* 2010; 24(3):401–7. [PubMed: 20075971]

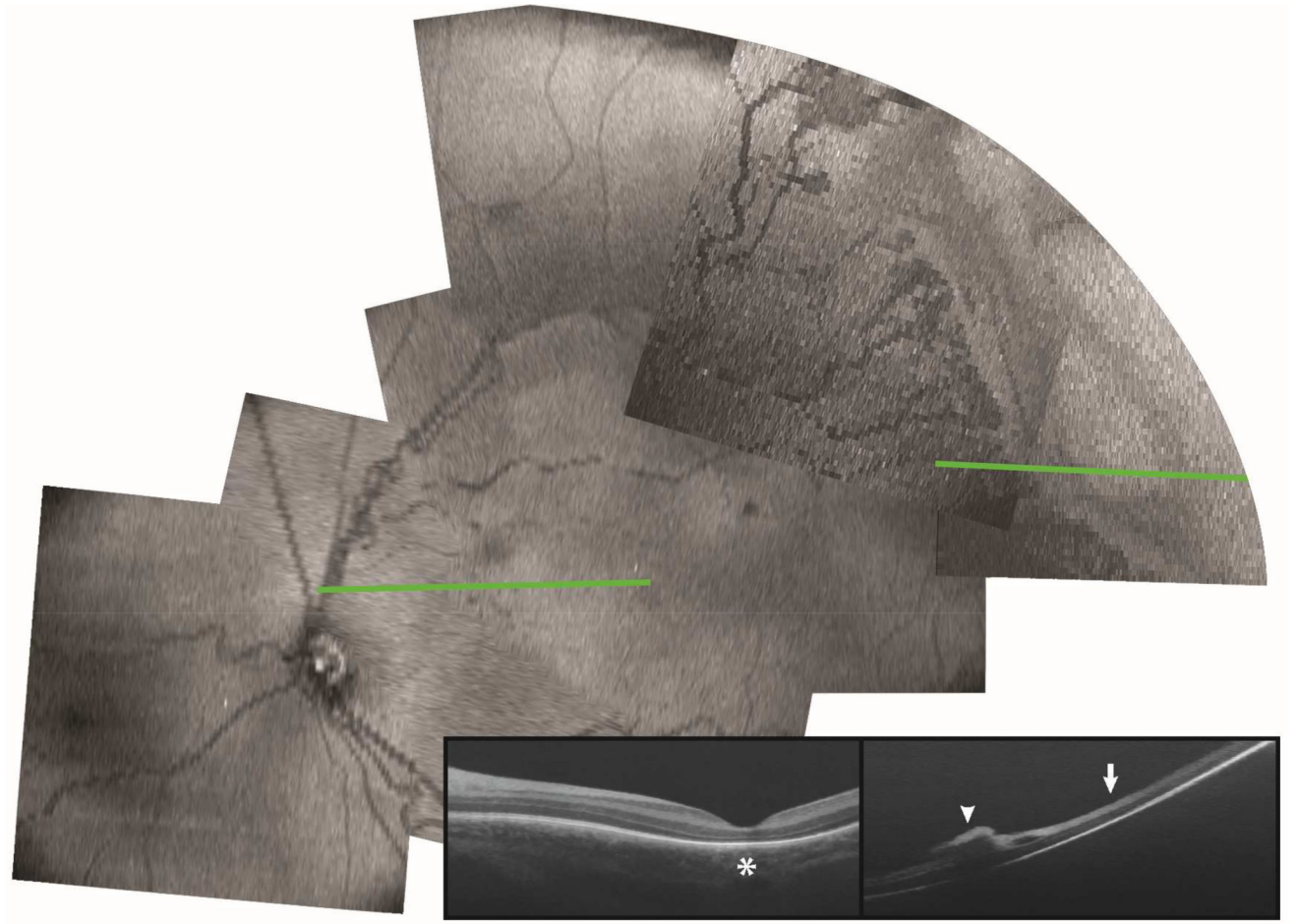


Figure 1. *En face* view and representative OCT B-scan of posterior pole and temporal retina in a preterm infant with zone II stage 3 ROP at the time of ROP screening examination. B-scan at the macular area (green line, left) showed absence of subfoveal photoreceptor ellipsoid zone (left panel, star). B-scan at the temporal retinal periphery (green line, right) showed preretinal neovascular tissue (right panel, arrowhead), inner retinal split, and inner retinal thickening (right panel, arrow).

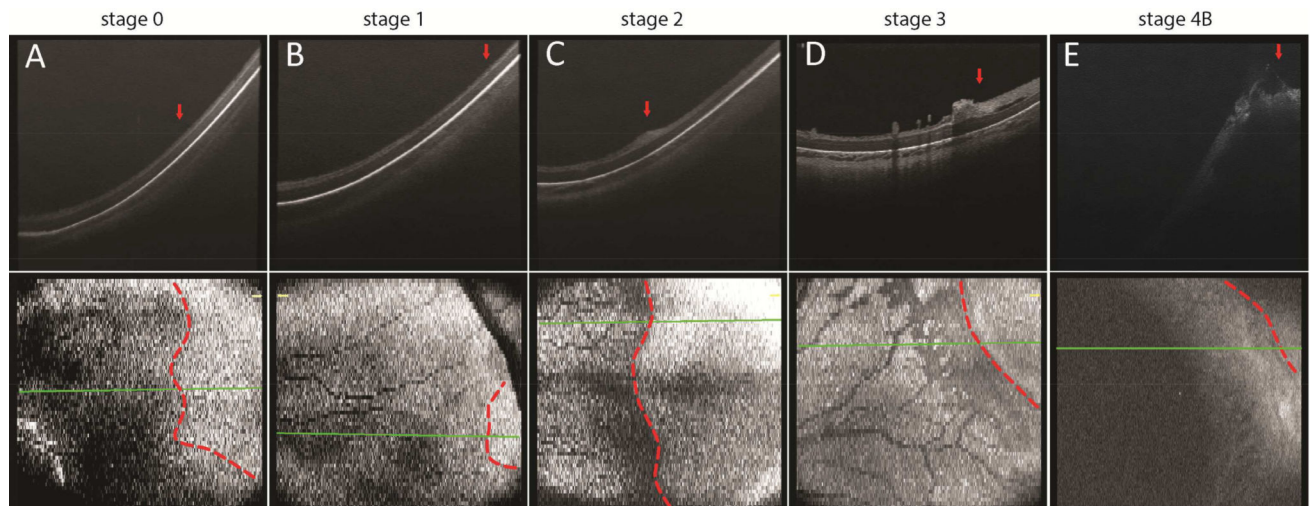


Figure 2.

Representative OCT B-scan and *en face* images across the vascular-avascular junction in the temporal peripheral retina in preterm infants with zone I stage 0 (A), zone II stage 1 (B), zone I stage 2 (C), zone I stage 3 (D), and zone I stage 4B (E) ROP. The vascular-avascular junction was delineated on the *en face* retina view (bottom panel, dotted line) and its respective position marked on the B-scan image (top panel, arrow). The retinal and choroidal thickness at the vascular-avascular junction on these B-scans, as well as retinal thickness 1000 μm anterior or posterior to the vascular-avascular junction are shown in Supplementary Table 1.

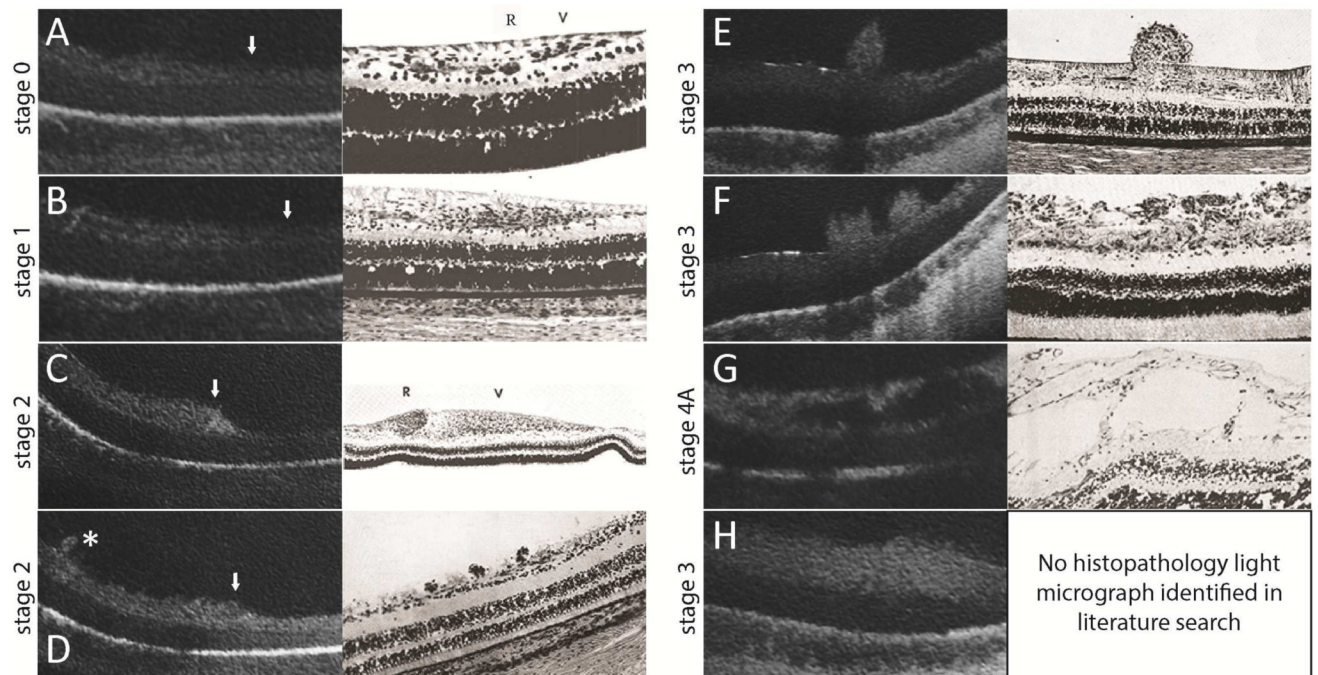


Figure 3.

SDOCT images (left) are correlated with historic representative light micrographs (right) at the vascular-avascular junction (A–D, white arrowhead with vascularized retina on the left side of the images) or adjacent to the vascular-avascular junction (E–G, posterior, and H, anterior) in eyes with ROP. **A:** Stage 0 ROP: in vascularized retina a faint hyporeflective band divided the inner retinal hyperreflective layer which gradually tapered to a single hyperreflective band in avascular retina. This was comparable to the normal angiogenesis pattern reported by Foos³¹ (adapted image), although the retinal layers were not as evident on OCT imaging compared to histopathology studies. **B:** Stage 1 ROP: a similar three-layered inner retina on the left gradually tapered to a one-layered structure in avascular retina. Similar to Foos³¹, the total thickness of the vascularized retina appeared to be greater than in stage 0 ROP.³¹ (also see Supplementary Table 1 thicknesses) **C:** Stage 2 ROP: pronounced thickening at the vascular-avascular junction was consistent with the ridge structure with hypertrophied anterior vanguard and posterior rear guard cells reported by Foos³¹. As with all OCT imaging, specific cellular elements could not be distinguished. **D:** Small neovascular buds, not noticed on clinical examination, could be seen on OCT in stage 2 ROP (asterisk). This was similar to the small elevations on the retinal surface observed by Reese,²⁸ which were presumed to be early endothelial proliferation. **E, F:** Stage 3 ROP: neovascular buds (E) and bands (F) frequented the preretinal surface. Their configurations were also consistent with neovascular findings reported by Reese.²⁸ **G:** Stage 4A ROP: there were schisis-like changes in the inner retinal layers posterior to the presumed area of retinal detachment. These schisis-like changes were often cavitory, and appeared similar to the large cystic spaces in the nerve fiber layer in later stages of proliferative disease reported by Kushner.³³ **H:** In stage 3 or 4 ROP, there was often diffuse thickening of the inner retinal layer of avascular retina. No correlating histopathology light micrograph was identified in our literature search.

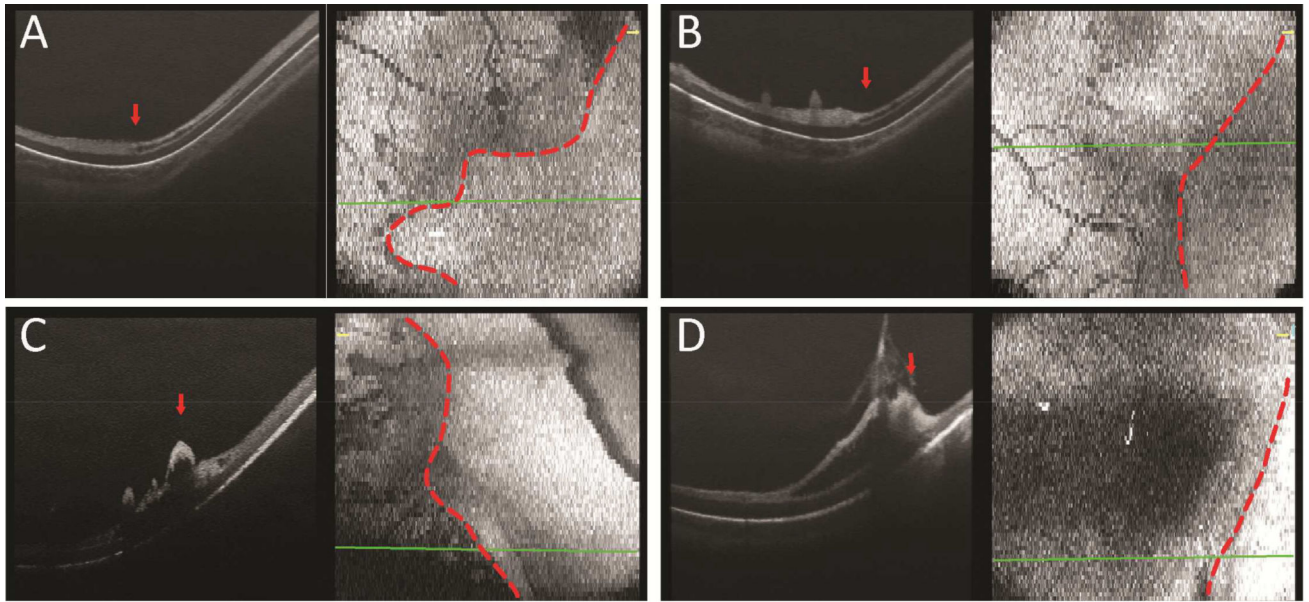


Figure 4. Representative OCT B-scan and *en face* images of the temporal retina in preterm infants with stage 3 ROP, with an inner retinal split, a hyporeflective lucency within the inner hyperreflective band, anterior to (A), at (B), and posterior to (C) the vascular-avascular junction. Focal vitreoretinal traction was also observed in some eyes with stage 3 ROP (D).

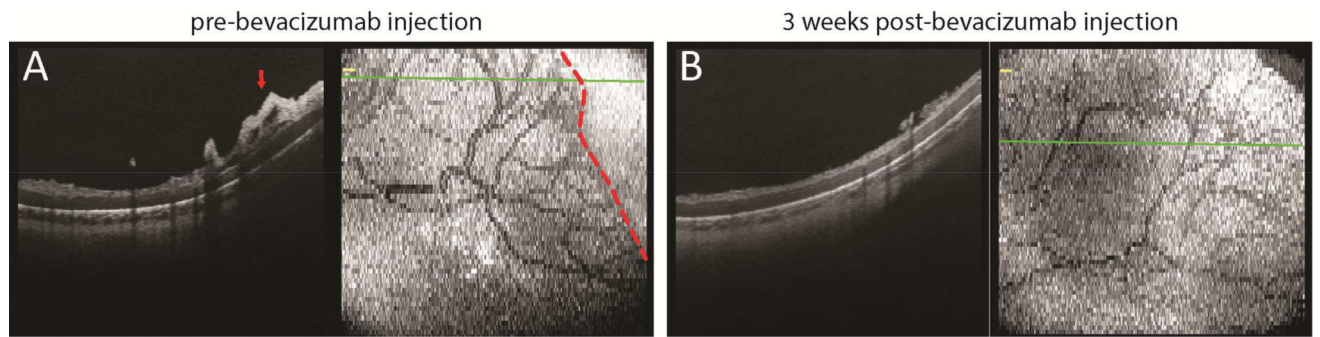


Figure 5. Representative OCT B-scan and *en face* images of the temporal retina in a preterm infant with zone I stage 3 ROP, prior to (A) and three weeks after (B) intravitreal bevacizumab injection, showing regression of preretinal neovascular elevations and further vascularization of the previously avascular retina compared to images in (A).

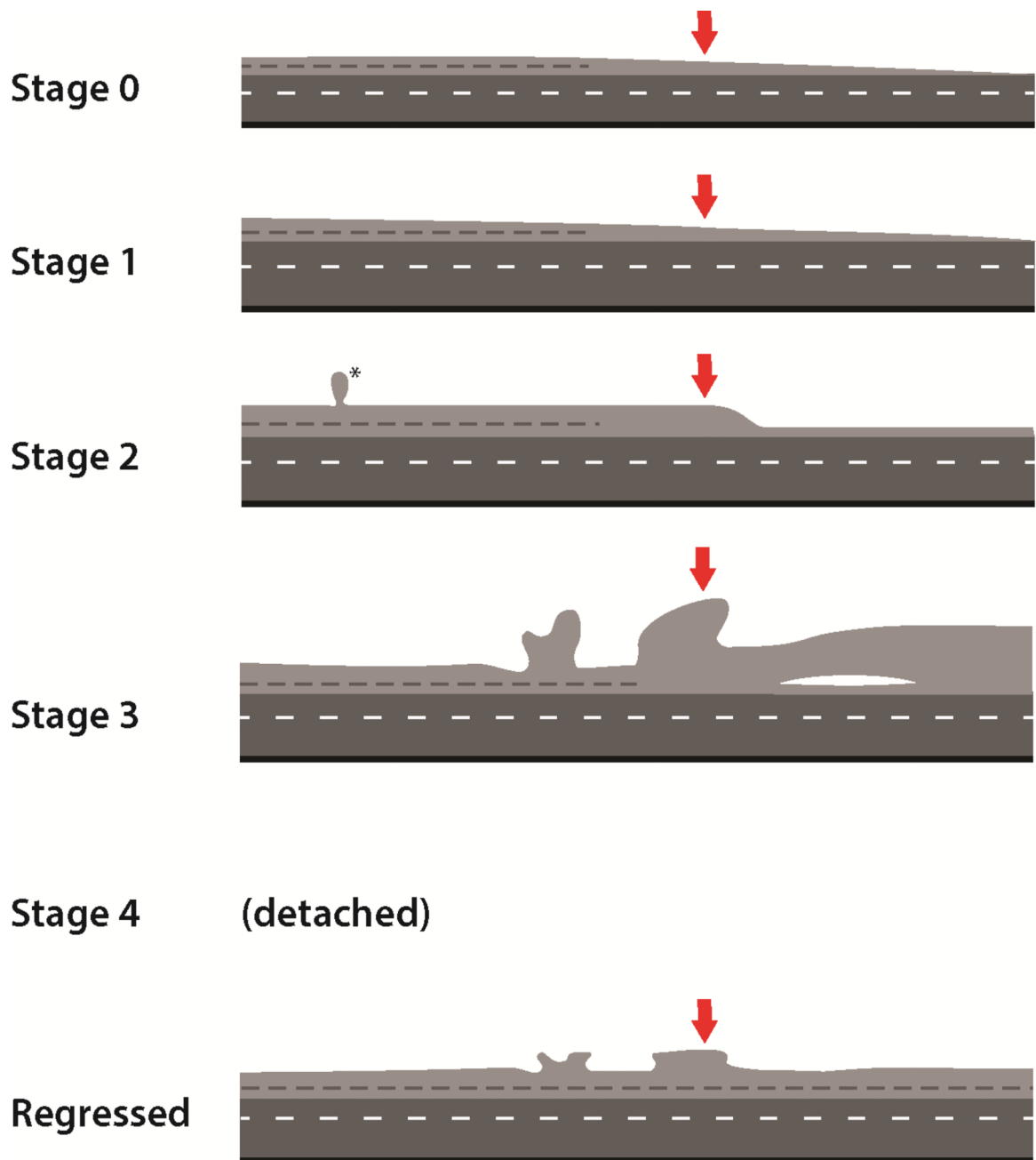


Figure 6. Schematic model of retinal development at the vascular-avascular junction on OCT imaging during different stages of ROP. The dash lines represent retinal layers observed on OCT: white dash line corresponds to outer plexiform layer and grey dash line represents the inner retinal hyperreflective band.

Demographics and clinical information of the preterm infants imaged at bedside with handheld, portable spectral-domain optical coherence tomography (SDOCT), including stage and zone of retinopathy of prematurity (ROP) and any ROP treatment

Table 1

Eye#	Baby#	Eye	Gestational age (weeks)	Birth weight (g)	Race	Sex	Age ^a at examination and imaging (weeks)	ROP Stage	Prior treatment
1	1	R	25	640	L	M	32	Z1S0	None
2	1	L	25	640	L	M	32	Z1S0	None
							34	Z1S2	None
							35	Z1S2	None
3	2	R	26	790	A	F	32	Z1S3R ^b	IVB ^d
							32	Z2S1	None
4	3	R	24	624	AA	M	32	Z1S3	None
							39	Z2S3R	IVB
5	4	L	23	475	M	F	34	Z1S3	None
							38	Z1S3R	IVB
6	4	R	23	475	M	F	41	Z2S3R	IVB
7	5	R	25.4	NA ^c	AA	M	35	Z2S3	None
8	5	L	25.4	NA	AA	M	35	Z2S3	None
							40	Z2S3R	Laser
9	6	L	23.8	650	C/L	F	33	Z1S3R	IVB
10	7	R	22	590	C	M	40	Z1S3R	IVB
							42	Z1S3R	IVB
							44	Z1S3R	IVB
11	7	L	22	590	C	M	40	Z1S3R	IVB
							42	Z1S3R	IVB
12	8	R	23	420	AA	F	41	Z1S4A	Laser/IVB
13	8	L	23	420	AA	F	42	Z1R	Laser/IVB
14	9	R	24.6	644	AA	F	33	Z1S3	IVB
15	9	L	24.6	644	AA	F	33	Z1S3	IVB
16	10	R	24	640	AA	F	39	Z2S4A	Laser/IVB

Eye#	Baby#	Eye	Gestational age (weeks)	Birth weight (g)	Race	Sex	Age ^a at examination and imaging (weeks)	ROP Stage	Prior treatment
17	10	L	24	640	AA	F	39	Z2S3R	Laser/IVB
							40	Z2S3R	Laser/IVB
							44	Z2S3R	Laser/IVB
							48	Z2S3R	Laser/IVB
18	11	R	25	NA	AA	M	39	Z2S4B	Laser

^a Postmenstrual age = gestational age + postnatal age

^b R: regressed

^c NA: not available/unknown

^d IVB: intravitreal bevacizumab injection